Supporting Information

Liquid phase exfoliation of MoS_2 and WS_2 in aqueous ammonia and their application in highly efficient organic solar cells

Begimai Adilbekova [a], Yuanbao Lin [a], Emre Yengel [a], Hendrik Faber [a], George Harrison [a], Yuliar Firdaus [a], Abdulrahman El-Labban [a], Dalaver H. Anjum [b], Vincent Tung [a], Thomas D. Anthopoulos [a,*]

Corresponding Authors

Professor Thomas D. Anthopoulos

Email: thomas.anthopoulos@kaust.edu.sa

[a] *King Abdullah University of Science and Technology (KAUST), KAUST Solar Center (KSC), Thuwal 23955, Saudi Arabia.*

[b] *Khalifa University, Department of physic, Abu Dhabi, United Arab Emirates.*

SI-1. PL measurements

We used a Horiba Fluorolog system with the excitation wavelength of 447 nm to perform PL measurements of the dispersions with MoS_2 and WS_2 nanosheets. As can be seen from the spectrum in **Fig. S1a**, MoS_2 dispersion showed a PL emission at around 660 nm corresponding to 1.89 eV.[1] On the other hand, in the PL spectrum of WS_2 dispersion in **Fig. S1b**, we observe a peak at around 645 nm (1.92 eV), corresponding to A excitonic absorption.[2] PL emission intensity for MoS_2 and WS_2 flakes shows a strong dependence on the thickness, so that the monolayer flakes of both materials exhibit a strong emission, which dramatically drops for multilayer flakes.[1, 2] Therefore, sufficiently strong emission arisen from MoS_2 and WS_2 nanosheets may have suppressed peaks from multilayer nanosheets in the dispersion.

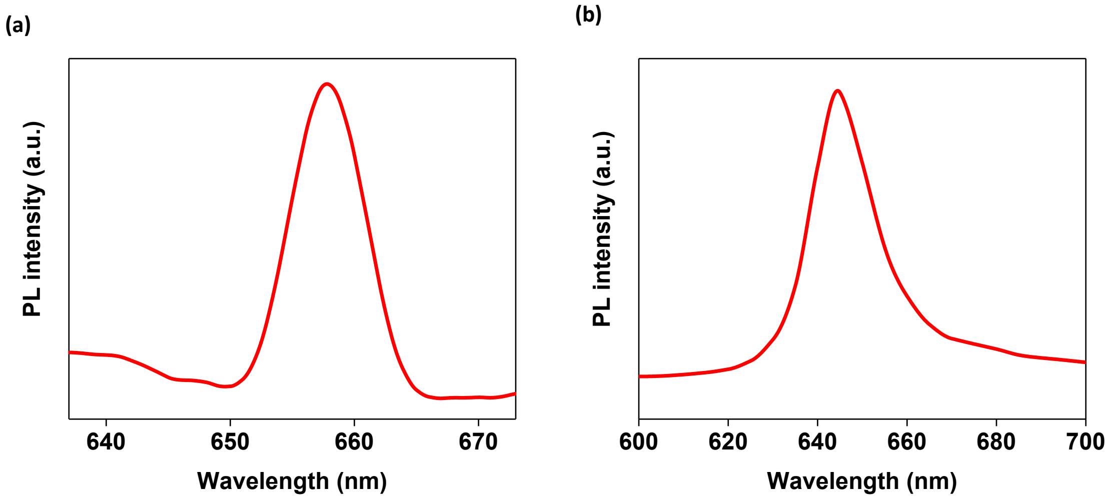

Fig. S1 Photoluminescence (PL) spectra of (a) MoS_2 and (b) WS_2 solutions performed in Fluorolog at 480 nm excitation.

SI-2. Device characterization

For the J–V measurements, we employed Keithley 2400 source meter and Oriel Sol3A Class AAA solar simulator (1 sun, AM1.5G), calibrated with a KG-5 silicon reference cell certified by Newport. The measurements of the devices were carried out in the N_2 filled glove box. External quantum efficiency (EQE) was characterized using an EQE system (PV measurement Inc.).

To investigate the effect of the concentration of MoS_2 and WS_2 flakes in the dispersions (determined by the centrifugation speeds), we fabricated a series of solar cells. Representative J-V curves of OSCs based on WS_2 and MoS_2 HTLs grown from solutions prepared at different centrifugation speeds, are shown in **Fig. S2**, while a summary of the photovoltaic parameters is given in **Table S1**. As can be seen, solutions with concentration of ≈0.5 mg mL^{-1} for MoS_2 (prepared at 6000 rpm), and ≈1 mg mL^{-1} for WS_2 (prepared at 4400 rpm), yield the best performing solr cells.

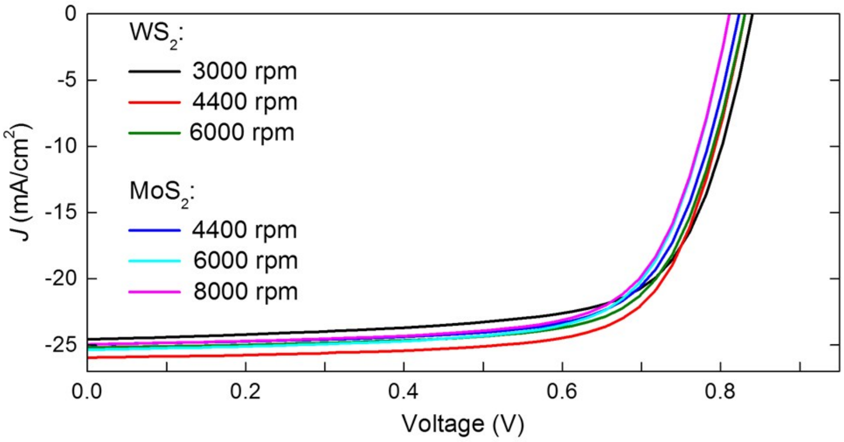

Fig. S2 J-V characteristics of PBDB-T-2F:Y6:PC$_{71}$BM based OSCs with WS_2 and MoS_2 prepared at different centrifugation speeds.

Table S1 Solar cell parameters of devices with WS_2 and MoS_2 HTLs with different concentrations based on different centrifugation speed measured under standard solar illumination of AM 1.5G.

HTL	Centrifuge speed (rpm)	Concentration (mg mL^{-1})	V_{OC} (V)	J_{sc} (mA cm^{-2})	FF	PCE (%)
WS_2	3000	1.2	0.84	24.6	0.70	14.5
	4400	1.0	0.83	26.0	0.72	15.6
	6000	0.9	0.83	25.2	0.72	15.0
MoS_2	4400	0.6	0.82	25.0	0.71	14.6
	6000	0.5	0.81	25.3	0.71	14.9
	8000	0.4	0.81	24.9	0.71	14.4

MoS_2 and WS_2 dispersions with different concentrations are used for the device fabrication to investigate the effect of the concentrations depending on the centrifugation speeds of the dispersions. J-V curves of OSCs with WS_2 and MoS_2 HTLs prepared at different centrifugation speeds are given in **Fig. S2**. As can be seen from the summarized photovoltaic parameters in **Table S1**, ≈0.5 mg mL^{-1} for MoS_2 (prepared at 6000 rpm) and ≈1 mg mL^{-1} for WS_2 (prepared at 4400 rpm) result in better performances.

SI-3. UPS measurement

UPS spectra collected from the bare ITO and films of 2D MoS_2 and WS_2 deposited onto ITO are given in. It is apparent in **Fig. S3a** from the secondary electron cut-off (21.22 eV) that upon deposition of TMDs the measured work function shows an increase to 5.04 eV and 5.1 eV for MoS_2 and WS_2, respectively, compared to ITO 4.7 eV. In **Fig. S3b** the higher kinetic (lower binding energy) region displays the valence region. While ITO demonstrates a valence band maximum (VBM) of 3.18 eV from a linear fit from the onset, a small peak like feature present in 2D MoS_2 and WS_2 is identified as the highest valence band component centred at 2.2 eV. The onset of this feature using a linear extrapolation leads to VBM 1.04 eV and 0.89 eV as is shown in the inset. When the spectrum is viewed in a log intensity, the intersection between the background and the onset is defined at 0.6 and 0.4 eV. These values are identified and could be interpreted as a band-tail state (0.4 eV higher in energy) in analogy to the UPS analysis by Kim et al. on CuSCN.[3] A theoretical density of state study is required to confirm this. The ionization energy for 2D MoS_2 and WS_2 can be assigned here as 6.08 eV and 5.99 eV from the vacuum. The summarized UPS data is given in **Table S2** and **Fig. S4**.

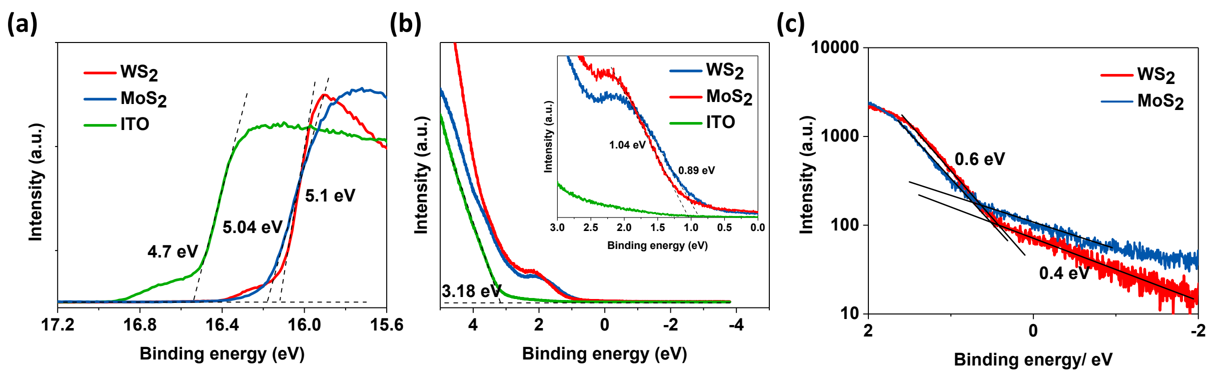

Fig. S3 (a-b) UPS spectra of bare ITO, ITO/WS_2, and ITO/MoS_2.

Table S2 Summary of UPS data for bare ITO, ITO/MoS_2 and ITO/WS_2.

Electrode	WF (eV)	VBM (eV)	IE (eV)
ITO/MoS_2	5.04	1.04	6.08
ITO/WS_2	5.1	0.89	5.99
ITO	4.7	3.18	8.88

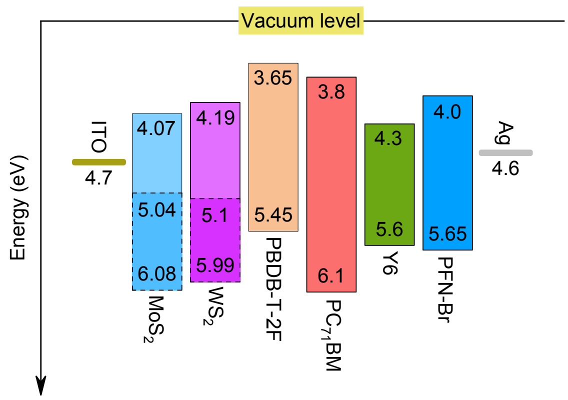

Fig. S4 Schematic showing band alignment of the solar cell with MoS_2 and WS_2.[4] Work function (WF), VBM and bandgap values of ITO, MoS_2 and WS_2 are extracted from UPS and PL data.

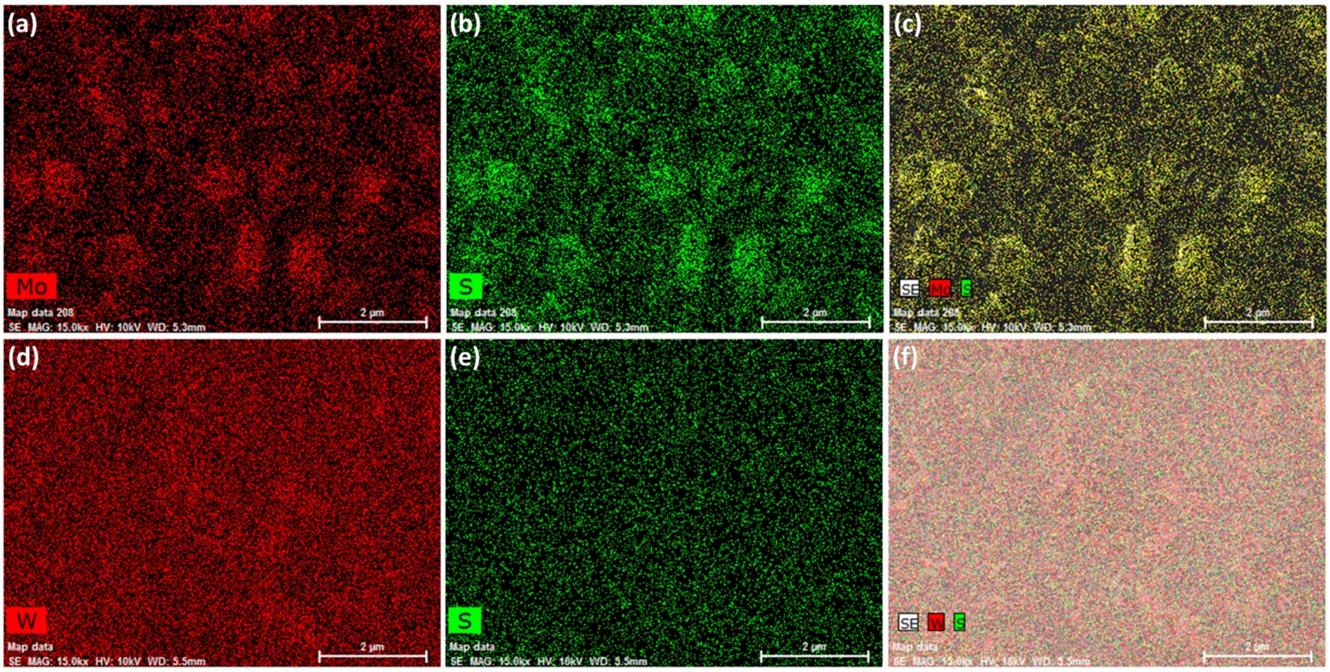

Fig. S5 Elemememental mapping of ITO surface after the deposition of (a-c) MoS_2, and (d-f) WS_2, obtained via EDS (SEM).

S4. References

1. Q. H. Wang, K. Kalantar-Zadeh, A. Kis, J. N. Coleman and M. S. Strano, *Nat Nanotechnol*, 2012, **7**, 699-712.
2. W. Zhao, Z. Ghorannevis, L. Chu, M. Toh, C. Kloc, P. H. Tan and G. Eda, *ACS Nano*, 2013, **7**, 791-797.
3. M. Kim, S. Park, J. Jeong, D. Shin, J. Kim, S. H. Ryu, K. S. Kim, H. Lee and Y. Yi, *J Phys Chem Lett*, 2016, **7**, 2856-2861.
4. Y. B. Lin, B. Adilbekova, Y. Firdaus, E. Yengel, H. Faber, M. Sajjad, X. P. Zheng, E. Yarali, A. Seitkhan, O. M. Bakr, A. El-Labban, U. Schwingenschlogl, V. Tung, I. McCulloch, F. Laquai and T. D. Anthopoulos, *Adv Mater*, 2019, **31**, 1902965.